JOURNAL OF MATERIALS SCIENCE 33 (1998) 1991–1995

Role of Mn in controlling the dielectric loss and ageing effect in $Pb(Zn_{1/3}Nb_{2/3})O_3$–$Pb(Fe_{2/3}W_{1/3})O_3$–$Pb(Fe_{1/2}Nb_{1/2})O_3$

R. NATARAJAN*, J. P. DOUGHERTY
Center for Dielectric Studies, Materials Research Laboratory, The Pennsylvania State University, University Park, PA 16802-4801, USA

Compositions in the $Pb(Zn_{1/3}Nb_{2/3})O_3$–$Pb(Fe_{2/3}W_{1/3})O_3$–$Pb(Fe_{1/2}Nb_{1/2})O_3$ (PZN–PFW–PFN) system show a high dielectric constant, insulation resistance and bend strength. In addition they can be sintered at very low temperatures. Hence they find technological applications as multilayer capacitors with low cost Ag-based internal electrodes. The dielectric loss in these ceramics was controlled by doping with Mn in the form of Mn-acetate, MnO_2, and $Pb(Mn_{1/3}Nb_{2/3})O_3$. The subtle differences in the dielectric properties of PZN–PFW–PFN, when Mn is taken in these forms are reported in this paper. A possible way of controlling the ageing effect is highlighted. © *1998 Chapman & Hall*

1. Introduction

Compositions in the system $Pb(Fe_{1/2}Nb_{1/2})O_3$–$Pb(Fe_{2/3}W_{1/3})O_3$ (PFN–PFW) can be sintered at temperatures ~950 °C and show a high dielectric constant (>20 000) with a T_{max} around room temperature [1–3]. These parameters are of technological importance for multilayer capacitor applications. However, the main disadvantage of the system is its high dissipation factor (>5%) and low resistivities [$<10^8$ Ω-cm]. With the addition of $Pb(Zn_{1/3}Nb_{2/3})O_3$ (PZN), there is a significant increase in resistivity and bend strength [1–3]. A reduction in the firing temperature to ~850 °C is also achieved with the PZN addition. This facilitates the use of cheaper Ag based internal electrodes for multilayer capacitor (MLC) applications [1–3]. Compositions in the PZN–PFN–PFW system also have fundamental significance from the point of view of structure–property correlation studies [4]. It is now well-established that the diffuse phase transition behaviour of relaxor ferroelectrics originates from its typical microstructure exhibiting micropolar regions of 1 : 1 ordering on the B-site sublattice dispersed in a disordered matrix [5]. Different compositions among the $Pb(B'_xB''_{1-x})O_3$ family exhibit different degrees of ordering in the B-site sublattice. PFW exhibits long range ordering of the B-site cation and no ferroelectricity is observed [4, 5]. In PFN, the B-site cations are largely disordered and normal ferroelectricity is observed. On the other hand, the short range order found in PZN type materials led to dispersion in the dielectric constant and relaxor ferroelectric behaviour. Hence study of dielectric properties in the PZN–PFN–PFW ternary system should shed more light on the understanding of the structure–property relations in these materials. For the present study, $(PZN)_{0.16}$–$(PFN)_{0.48}$–$(PFW)_{0.36}$ is chosen because the T_{max} of this composition is around room temperature [1–3]. The unique nature of small amounts of doped Mn in improving significantly the properties of many of the electroceramic products such as PTC elements, varistor, and capacitors is well documented [4, 7–9]. To understand the role played by Mn in controlling the dielectric properties and ageing phenomena observed in Mn doped relaxor ferroelectrics [10, 11], Mn is doped in three different forms. It is used in the form of Mn-acetate, MnO_2, and as equivalent amount of $Pb(Mn_{1/3}Nb_{2/3})O_3$ (PMN). This paper describes the dielectric properties of PZN–PFN–PFW modified with Mn in these forms. Also, a possible way of reducing the ageing effect is highlighted. Mn-doped in the form of Mn-acetate, MnO_2, and PMN are designated in this paper as xMnA, xMnOX, and xPMN, respectively (where x is the mol%).

2. Experimental procedures

Reagent grade PbO, ZnO, Nb_2O_5, Fe_2O_3, and WO_3 with purities greater than 99.5% were mixed in the correct stoichiometric ratios for 24 h in a vibratory mill using ethyl alcohol and zirconia as the grinding media. The oven-dried powder was crushed and calcined at 750 °C for 4 h. Different amounts (0.1–0.85 mol %) of the Mn-compound taken as acetate, MnO_2, or PMN were added to the calcined powder which was once again, vibratory milled for 24 h. The PMN powder was separately prepared using the columbite method [12]. After drying, the powders

---

* *Permanent address*: C-MET, Dept. of Electronics, Trichur, India-680 771.

were pressed into pellets and sintered at 850 °C for 1 h. Different cooling rates, ranging from quenching to 1.5 °C min^{-1} were employed. All the sintered samples were found to have a $\geqslant$93% sintered density. Gold electrodes were sputtered onto the ceramic for electrical contact. The dielectric properties were measured using an HP 4274A LCR meter under computer control in the frequency range from 0.1–100 KHz. The measuring field was less than 10 V cm^{-1}. A Delta design model 2300 environmental chamber was used for the measurement of the dielectric constant (K) as a function of temperature (T). Prior to the measurements all the samples were kept in the oven at 150 °C for 8 h and the dielectric measurements were measured from high temperature to low temperature at a rate of 2 °C min^{-1}. For the dynamic ageing study, samples were aged at 20 °C. In the study of the K–T behaviour of "aged" samples, they were introduced into the environmental chamber at a temperature far below the ageing temperature. Measurements were performed from low temperature to high temperature at a rate of 2 °C min^{-1}.

X-ray diffraction patterns were recorded with a Scintag X-ray diffractometer using CuK_α radiation. The content of the pyrochlore structured phase in the sample was obtained using the relation:

$$\text{Pyrochlore content} = \frac{I_{\text{pyro}}(222)}{I_{\text{pyro}}(222) + I_{\text{perov}}(110)} \times 100\% \tag{1}$$

where $I_{\text{pyro}}(222)$ is the intensity of the (222) pyrochlore X-ray peak and $I_{\text{perov}}(110)$ is the intensity of the (110) X-ray peak of the perovskite structured phase in the investigated sample. The microstructures of the samples were analysed using an ISI DS 130 scanning electron microscope.

3. Results

3.1. Dielectric properties

Fig. 1a shows the X-ray diffraction pattern of undoped $(PZN)_{0.16}$–$(PFN)_{0.48}$–$(PFW)_{0.36}$ calcined at 750 °C for 4 h. The content of the pyrochlore structured phase in this powder was found to be $\simeq$11%. However, when the sample is sintered at 850 °C for 1 h this value dropped to $\leqslant$2% (Fig. 1b). For the sample doped with Mn and sintered at 850 °C for 1h the pyrochlore content was found to vary with the form of the Mn addition. For the range of dopant content studied, the pyrochlore content of the xMnOX samples is ~3%, and for the xMnA samples it is ~4%. However, for the xPMN samples, there was no increase in the pyrochlore content, and it remained equivalent to that of undoped samples. Fig. 2(a–c) show the microstructure of the undoped and doped ceramics. Irrespective of the form and amount of the Mn-addition, the microstructures of all the ceramics look similar with an average uniform grain size of ~4–4.5 μm. The K–T curve for the undoped ceramic is shown in Fig. 3. These ceramics exhibit a $K_{\max} \sim 9\,000$ with a $T_{\max} \sim 30$ °C. The K–T curves are broad and diffuse with the diffuseness, measured between 1 and 100 KHz, being ~5.5 °C. This value is low compared to that of typical relaxor ferroelectrics such as PMN–PT or PZN–BT [10, 11]. As could be inferred from Fig. 3, the major disadvantage of this composition is its relatively unacceptable high loss, especially at higher temperatures. Figs 4–6 represent the typical K–T curves obtained in the cases of the Mn-doped ceramics. Table I summarizes the dielectric data obtained with the Mn-doping using different forms of Mn. In general, irrespective of the form of Mn taken the addition leads to: (i) a considerable decrease in the loss factor; (ii) a slight reduction in the K value and the percentage decrease increases with Mn content; (iii) a slight increase in $T_{\max}$ to ~35 °C, irrespective of the dopant content, from 0.1 to 0.85 mol % and (iv) the frequency dispersion of the K–T curves decrease with an increasing Mn content. All these results agree with the observations made in the case of Mn-doped PMN–PT and PZT–BT ceramics [10, 11].

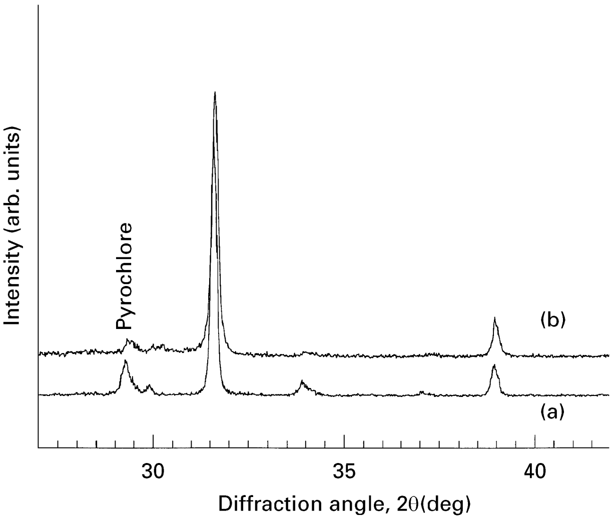

Figure 1 X-ray diffraction pattern of undoped $(PZN)_{0.16}$–$(PFW)_{0.36}$–$(PFN)_{0.48}$ (a) calcined at 750 °C for 4 h and (b) sintered at 850 °C for 1 h.

For a given dopant content, PMN samples show slightly higher K value compared to MnA and MnOX samples with the MnA samples displaying the smallest values. This correlates well with the amount of pyrochlore phase present in the ceramic. The diffuseness of the K–T curve persists even with higher Mn contents for xPMN samples. In the case of MnA samples the diffuseness decreases considerably at contents as low as 0.3 mol % (Fig. 5). The loss factor (tan δ) is well controlled in the MnA samples, particularly at higher temperatures (Table I). For the MnOX samples a sharp decrease in the diffuseness is observed at a slightly higher amount of 0.5% and the K values are in between those of the PMN and MnOX doped samples.

3.2. Ageing behaviour

As far as the dynamic ageing behaviour is concerned, the following general trend is observed with Mn doping; (i) an increase in the Mn content increases the ageing rate; (ii) at the temperature of ageing, a "saddle

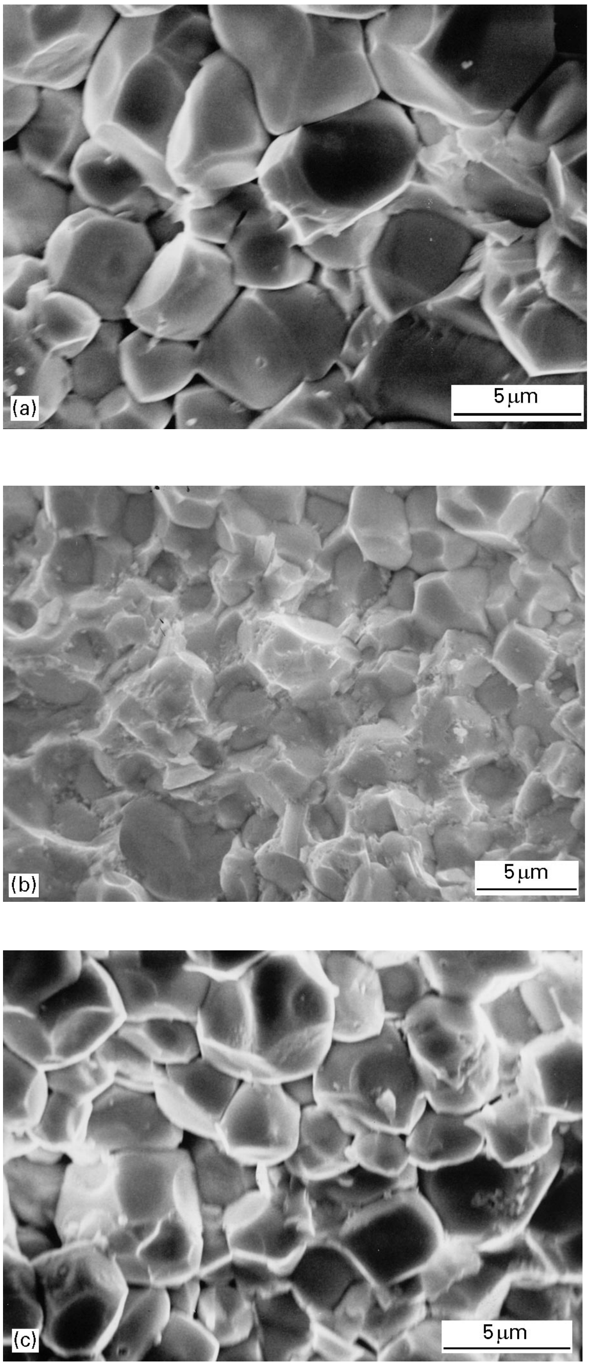

Figure 2 Microstructure of PZN–PFW–PFN sintered at 850 °C for 1 h with (a) 0.85MnA, (b) 0.85MnOX and (c) 0.85PMN.

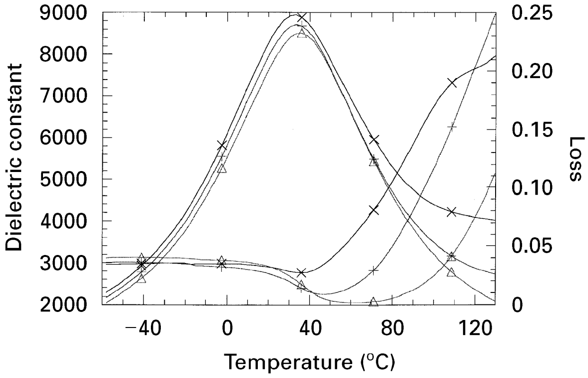

Figure 3 Dielectric constant and loss of the undoped PZN–PFW–PFN ceramic, measured at; (×) 1 K, (+) 10 K and (△) 100 K.

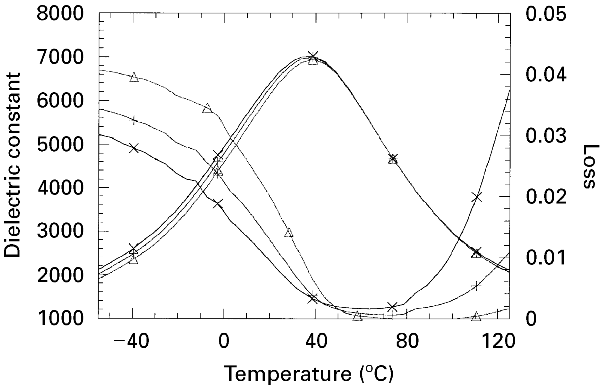

Figure 4 *K–T* curves for the PZN–PFW–PFN sample with 0.3PMN. Data collected at (×) 1 K, (+) 10 K and (△) 100 K.

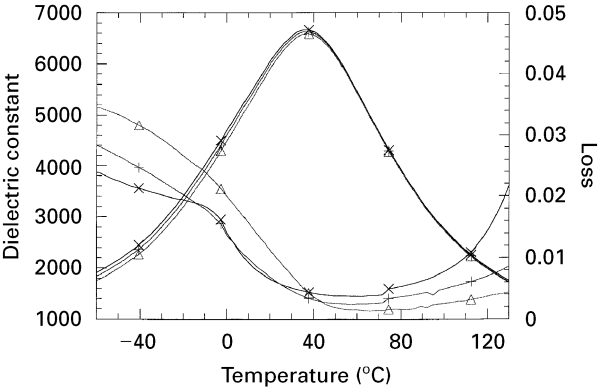

Figure 5 *K–T* curves for the PZN–PFW–PFN sample with 0.3MnA. Data collected at (×) 1 K, (+) 10 K and (△) 100 K.

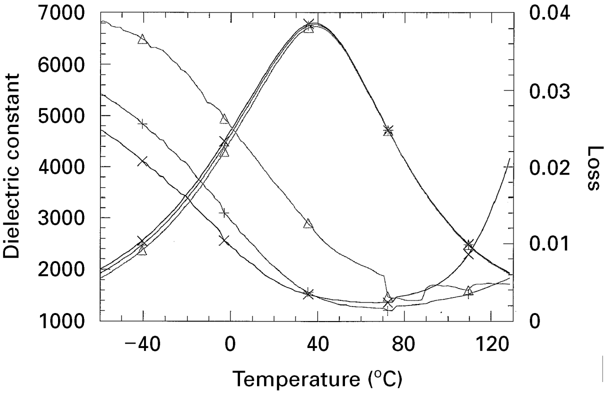

Figure 6 *K–T* curves for the PZN–PFW–PFN sample with 0.5MnOX. Data collected at (×) 1 K, (+) 10 K and (△) 100 K.

like" depression in the K–T and tan δ–T curves are observed; (iii) the frequency dispersion weakens and (iv) the low frequency component shows an increased ageing rate.

These observations agree with earlier reports [10–15]. The major difference in doping Mn in different forms arises in its ageing behaviour. As observed in Fig. 7, for a given dopant content even within 24 h of ageing the MnA samples show a much more pronounced ageing compared to the MnOX samples. For clarity, only the measurement taken at a 1 KHz frequency is shown in Fig. 7. On the other hand, when

TABLE I Dielectric data for PZN–PFW–PFN samples doped with Mn additions

Dopant content (%)	K_{max}	tanδ (%) at			ΔT_{max} between 1 and 100 KHz	Resistivity (Ω cm)
		−55 °C	30 °C	125 °C		
0	9000	2.6	2.2	21.0	5.5	3.89×10^{8}
0.1 PMN	7400	3.2	0.66	12.3	2.8	1.74×10^{11}
0.2 PMN	7300	3.0	0.55	6.9	2.6	1.72×10^{11}
0.3 PMN	7000	2.9	0.50	3.7	2.2	2.28×10^{11}
0.5 PMN	6920	2.5	0.60	2.4	2.0	2.10×10^{11}
0.1 MnA	7000	3.3	1.2	6.2	1.7	4.65×10^{11}
0.3 MnA	6600	2.1	0.46	1.8	0.96	4.74×10^{11}
0.5 MnA	5800	1.9	0.88	1.2	0	3.16×10^{11}
0.85 MnA	5700	1.1	1.0	1.1	0	3.04×10^{11}
0.1 MnOX	7250	3.1	1.9	9.2	2.8	4.05×10^{11}
0.3 MnOX	6920	2.0	0.22	2.8	2.1	4.64×10^{11}
0.5 MnOX	6850	2.1	0.34	1.8	0.7	5.06×10^{11}
0.85 MnOX	6600	1.8	0.48	1.1	0	3.04×10^{11}

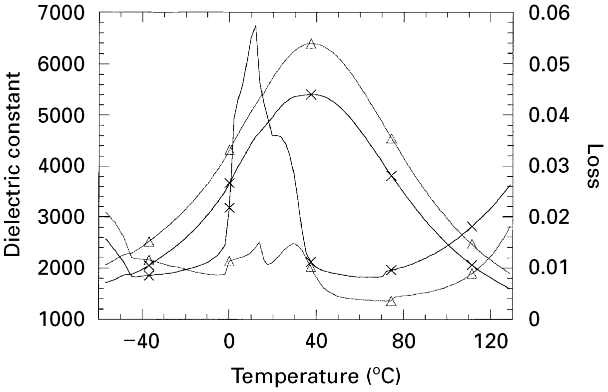

Figure 7 K–T curves at 1 KHz for 0.85% (×) MnA and (△) MnOX samples aged at 20 °C for 24 h.

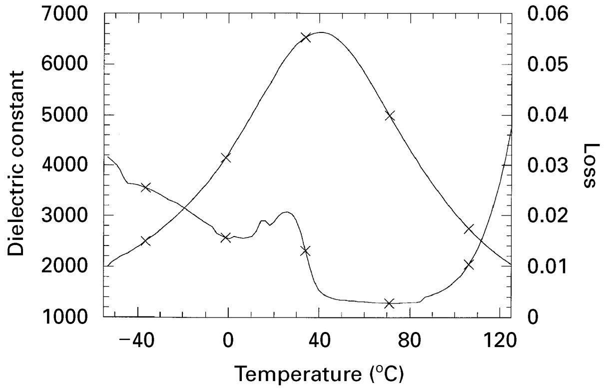

Figure 8 K–T curves at 1 KHz for the 0.3PMN sample aged at 20 °C for 1000 h.

doped as xPMN, samples show a considerably reduced ageing effect even after 1000 h of ageing (Fig. 8).

4. Discussion

The influence of temperature and frequency on the dielectric loss of relaxor ferroelectrics have been discussed by many authors [4, 16, 17]. The dielectric loss against temperature curve can be divided into three regions. In the low temperature region, the main contribution to loss arises from domain wall motion [16, 17]. Because of increased domain wall motion at higher frequencies an increase in frequency leads to a higher loss in this region. Just above the Curie temperature the loss becomes extremely low because of the absence of domains and also the temperature is not high enough for appreciable conductivity. As the temperature is increased, again an increase in the dielectric loss is observed. This is because of the increase in conductivity at higher temperatures [16, 17]. In the higher temperature region, low frequency components show an increased loss because of closer approximation to DC conductivity.

As shown in Fig. 3, the dielectric loss of the undoped ceramic is unacceptably high, especially at higher temperatures. As explained above, the loss arises from the increase in internal conductivity in this temperature range. The grain conductivity of undoped PZN–PFW–PFN has been shown to arise from an electron-hopping mechanism between Fe^{2+} and Fe^{3+} ions at the B-site [18]. For the temperature range used in the present study, Mn can exist as Mn^{2+} (with an ionic radius of 6.7 nm) and Mn^{3+} (5.8 nm) [10]. Hence Mn occupies the B-site, leading to acceptor doping which is compensated for by oxygen vacancies. The acceptor effect of Mn is also evident from the increase in resistivity observed, as shown in Table I. The unique effect of Mn doping in controlling the loss of normal and relaxor ferroelectrics is well-documented in the literature [4]. The oxygen vacancy compensation with Mn doping has also been observed in PMN and PMT–PT compositions [13–15].

A comprehensive review of the ageing studies in normal ferroelectrics can be found in reference [19]. The mechanism of the dynamic ageing effect in relaxor ferroelectrics such as observed in Mn doped PMN, PMN–PT, and PZN–BT ceramics is described in references [10–15]. Ageing is a process for a system to evolve from a nonequilibrium state to the equilibrium state. The microstructure of a relaxor ferroelectric contains ordered micropolar regions of different sizes [5]. Different regions have a different degree of ferroelectricity and Curie temperature, depending on the composition and size of the microregions. The polarization vectors in these microregions are unstable against KT and hence constantly switch between alternative orientation states. These different orientations of polarization will be of slightly differing energies because of microheterogeneity in the composition [5]. Hence the polarization vector will tend to spend longer times in the lowest energy minimum. In the case of the Mn-doped samples, oxygen vacancies form defect pairs with positively charged defect sites [14, 15]. The reorientation and alignment of the defect dipoles with the local polar domains affect the domain wall mobility as well as the dielectric response leading to ageing. The observed relatively low ageing effect when Mn is taken in the form of PMN can be explained as follows: when doped as PMN, the inherent stoichiometry of the composition is maintained. It is known that stoichiometric and pure PMN, PMN–PT samples do not exhibit ageing [13–15]. Only the impure and acceptor doped samples show the ageing effect. Hence maintaining stoichiometry could be a possible explanation for the low ageing effect observed in xPMN samples. Further studies such as electron paramagnetic resonance investigations are being carried out to probe the relation between the oxidation state of Mn and the observed dielectric phenomena.

5. Conclusions

PZN–PFW–PFN compositions exhibit a high dielectric constant and the loss factor is very high. Small amounts of Mn taken in the form of MnA, MnOX and PMN was found to be effective in controlling the loss. MnA samples showed good control over the loss especially at high temperature. For a given amount of dopant, PMN samples showed a higher K value and the diffuse nature of the dielectric behaviour remained. The dynamic ageing rate of the xPMN samples are very low compared to those of the xMnA and xMnOX samples. Maintaining stoichiometry could be a possible way to reduce the ageing effect.

Acknowledgement

One of the authors, Raghu Natarajan, wishes to thank the Ministry of Science and Technology, Government of India, for financial support.

References

1. M. YONEZAWA, K. UTSUMI, A. OCHI and T. MORI, in Proceedings of the 7th International Symposium on Applications of Ferroelectricity, (IEEE, 1990) p. 159.
2. M. YONEZAWA, M. MIYAUCHI, K. UTSUMI and S. SAITO, in "High technology ceramics", edited by P. Vincenzini, (Elsevier, 1987), p. 1493.
3. M. YONEZAWA, *Amer. Ceram. Soc. Bull.* **62** (1983) 1375.
4. R. E. NEWNHAM and S. TROLIER-MCKINSTRY, *Ceram. Trans.* **32** (1992) 1.
5. L. E. CROSS, *Ferroelectrics* **76** (1987) 241.
6. T. R. SHROUT and J. P. DOUGHERTY, *Ceram. Trans.* **8** (1990) 3.
7. J. H. LEE, S. H. KIM and S. H. CHO, *J. Amer. Ceram. Soc.* **78** (1995) 1845.
8. T. R. N. KUTTY and P. MURUGARAJ, *Mater. Lett.* **3** (1985) 195.
9. N. RAGHU and T. R. N. KUTTY, *Appl. Phys. Lett* **60** (1992) 100.
10. X. WANG and X. YAO, *Ferroelectric* **154** (1994) 307.
11. W. Y. PAU, Q. S. JIANG and L. E. CROSS, *ibid.* **82** (1988) 111.
12. S. L. SWARTZ and T. R. SHROUT, *Mat. Res. Bull.* **17** (1982) 1245.
13. T. R. SHROUT, W. HUEBNER, C. A. RANDALL and A. D. HILTON, **93** (1989) 361.
14. W. Y. PAU, T. R. SHROUT and L. E. CROSS, *J. Mater. Sci. Lett.* **8** (1989) 771.
15. Q. M. ZHANG, J. ZHAO and L. E. CROSS, *J. Appl. Phys.* **79** (1996) 1.
16. H. K. HARDTL, *Ceram. Int.* **8** (1982) 121.
17. P. GERTHSEN, H. K. HARDTL and N. A. SCHMIDT, *J. Appl. Phys.* **51** (1980) 1131.
18. G. DRAZIC, H. TRONTELJ and D. KOLAR, *Mater. Sci. Engng.* **B26** (1994) 189.
19. W. A. SCHULZE and K. OGINO, *Ferroelectrics* **87** (1988) 361.

Received 24 March
and accepted 17 June 1997